Applied Clay Science 112–113 (2015) 25–31

Contents lists available at ScienceDirect

Applied Clay Science

journal homepage: www.elsevier.com/locate/clay

Research paper

Influence of interlayer functionalization of kaolinite on property profile of copolymer nanocomposites

Sonia Zulfiqar [a,b,*], Muhammad Ilyas Sarwar [a,c,**], Nagina Rasheed [c], Cafer T. Yavuz [d]

[a] Department of Chemistry, School of Natural Sciences (SNS), National University of Sciences and Technology (NUST), Islamabad 44000, Pakistan
[b] Institute for Polymer Materials, POLYMAT, University of the Basque Country (UPV-EHU), Joxe Mari Korta Center, Avda. Tolosa 72, 20018 Donostia–San Sebastian, Spain
[c] Department of Chemistry, Quaid-i-Azam University, Islamabad 45320, Pakistan
[d] Graduate School of EEWS, Korea Advanced Institute of Science and Technology, 335 Gwahangno, Yuseong-gu, Daejeon 305-701, Republic of Korea

ARTICLE INFO

Article history:
Received 31 August 2014
Received in revised form 8 April 2015
Accepted 14 April 2015
Available online 25 May 2015

Keywords:
Kaolinite
Nanocomposites
Electron microscopy
Mechanical properties
Thermal stability

ABSTRACT

Nanocomposites of co-poly (vinyl chloride–polyvinyl acetate–polyvinyl alcohol) (PVC–PVAc–PVA) and kaolinite were prepared via solution intercalation technique. To improve compatibility among the phases and to expand the interlayer basal spacing, kaolinite was modified using dimethylsulfoxide (DMSO) as a swelling agent. The influence of kaolinite dispersion and interaction between the disparate phases on the properties of nanocomposites were investigated using Fourier transform infrared spectrometer (FTIR), X-ray diffraction (XRD), scanning electron microscopy (SEM), transmission electron microscopy (TEM), mechanical testing, thermogravimetric analysis (TGA) and water absorption measurements. IR data confirmed the hydrogen bonds formed between DMSO and the surface hydroxyl groups of kaolinite. XRD and microscopic results revealed that clay mineral was intercalated with uniform dispersion at nanoscale in the matrix. Tensile testing of these materials indicated significant improvements in the mechanical properties relative to the pure copolymer. Incorporation of kaolinite into the organic phase enhanced the thermal stability of the nanocomposites. Water absorption of the nanomaterials was reduced upon the addition of modified kaolinite rendering decreased permeability with increasing dispersibility of clay mineral in the copolymer matrix.

1. Introduction

Nanocomposites are a unique and important class of nanomaterials produced from the ultimate blending of organic and inorganic phases at nanoscale (Alvi et al., 2014). Among the inorganic phases, clay minerals exhibit a pivotal role and the most widely exploited minerals are phyllosilicates, especially the smectites (Zahra et al., 2014). Intercalation is the prerequisite for complete delamination of silicate layers in the organic matrix, leading to the formation of nanocomposite materials (Alvi et al., 2013). Due to the ample swelling behavior, montmorillonite (Mt) is the most employed clay mineral for the fabrication of nanocomposites with potential high-tech applications (Theng, 1979; Alexandre and Dubois, 2000; Pinnavaia and Beall, 2000; Viville et al., 2003). It is believed that kaolinite is originally produced by chemical weathering of igneous rocks containing the feldspar and is an abundantly available clay mineral having chemical composition $Al_2Si_2O_5(OH)_4$ (Ruiz-Hitzky and Meerbeek, 2006). Kaolinite is a 1:1 layered dioctahedral aluminosilicate formed by silicon tetrahedral sheets and aluminum octahedral sheets. The individual layers are connected together by van der Waals and hydrogen bonds that limit the access to aluminol groups for grafting reaction. They are linked also by the strong dipole interactions between the asymmetric layers. As a result, kaolinite has been described as non-expandable for a long time, until it was revealed that some polar molecules could be intercalated into the interlayers of kaolinite. This clay mineral is an inexpensive additive that can improve the properties of materials (Bailey, 1988; Pinnavaia and Beall, 2000; Alkan et al., 2005; Turhan et al., 2010) and is widely used in industry as paper or cosmetics additive, and in ceramics. However, interlayers of kaolinite are not easily accessible; its interlayer chemistry is much less developed than Mt. Therefore, only few reports on kaolinite intercalation and nanocomposite formation are encountered in literature relative to Mt (Tomposon and Cuff, 1985; Ledoux and White, 1996; Cabeda et al., 2004; Alkan et al., 2008; Elbokl and Detellier, 2008; Li et al., 2008; Karaoglu et al, 2009; Mbey et al., 2012). Various swelling agents have been employed for kaolinite intercalation including DMSO, N-methylformamide (NMF), potassium acetate, hydrazine, urea, cyclic imides and methanol (Tomposon and Cuff, 1985; Uwins et al., 1993; Ledoux and White, 1996; Komori et al., 1998; Frost et al., 1999; Elbokl and Detellier, 2008).

Nanohybrid materials have been prepared from the grafting of 3-aminopropyltriethoxysilane onto the internal aluminol groups of

---

* Correspondence to: S. Zulfiqar, Department of Chemistry, School of Natural Sciences (SNS), National University of Sciences and Technology (NUST), Islamabad 44000, Pakistan. Tel.: +92 51 90855608; fax: +92 51 90855552.

** Correspondence to: M.I. Sarwar, Department of Chemistry, School of Natural Sciences (SNS), National University of Sciences and Technology (NUST), Islamabad 44000, Pakistan. Tel.: +92 51 90855578; fax: +92 51 90855552.

E-mail addresses: soniazulfiqar@yahoo.com (S. Zulfiqar), ilyassarwar@hotmail.com (M.I. Sarwar).

http://dx.doi.org/10.1016/j.clay.2015.04.010
0169-1317/

kaolinite previously intercalated with DMSO or urea. The modified kaolinite was coated on a platinum electrode as electrochemical sensors to leach out $[Ru(CN)_6]^{4-}$ anions through multi-sweep cyclic voltammetry. Similarly, a range of compounds bearing hydroxyl groups were successfully grafted onto the OH groups of kaolinite yielding amino-functionalized kaolinite derivative. These derivatives were robust nanohybrid materials, decomposing at temperatures above 300 °C and resisting hydrolysis (Tonle et al., 2007). A series of organic–inorganic nanohybrid materials have been achieved by the intercalation of ionic liquids based on imidazolium derivatives in the interlayer spaces of kaolinite. Intercalation with imidazolium salts augmented the thermal stability of the resulting materials by more than 150 °C with respect to DMSO–kaolinite intercalate. The observed high thermal stability is promising for the use of these nanohybrid materials as precursor for the synthesis of new nanocomposites by incorporation of polymer in kaolinite at high temperature (Letaief and Detellier, 2007). In another related attempt, electrical conductivity of kaolinite nanohybrid materials prepared from the intercalation of ionic liquids based on imidazolium derivatives was measured at various temperatures. The imidazolium cations aligned to form alternating tunnels of organic cations and halide anions resulted in the highest ionic conductivity in a temperature range of 160–200 °C. At higher temperatures, the conductivity dropped dramatically due to the decomposition of organic material and the resulting collapse of the structure. The conductivity trend was highly dependent on the structure of the imidazolium derivatives (Letaief et al., 2008). Kaolinite–PVC nanocomposites were fabricated by dispersing the nanolayers into PVC matrix by the solution intercalation method (Turhan et al., 2010). The organophilicity of kaolinite was improved when intercalated with DMSO. Thermal stability of the nanocomposites was improved and transparency was increased relative to pure PVC but reduced with increase in kaolinite in the nanocomposites.

Herein we report the synthesis and characterization of PVC–PVAc–PVA and modified kaolinite nanocomposites using solution intercalation technique. Intercalation of kaolinite was carried out with DMSO for ample compatibility between the organic and inorganic phases. Modified kaolinite is suitable as filler in the preparation of polymeric nanocomposites. Tetrahydrofuran (THF) was used as reaction solvent for the preparation of nanocomposites. Different compositions of the nanocomposites containing 1 to 20-wt.% modified kaolinite were prepared. Thin composite films obtained after evaporating the solvent were subjected to FTIR, XRD, TEM, SEM, TGA, tensile testing and water absorption measurements.

2. Experimental

2.1. Chemicals

Co-poly(vinylchloride–vinylacetate–vinylalcohol) with an average $M_n = 27{,}000$, having a composition of vinylchloride, vinylacetate, and vinylalcohol, 90, 4, and 6 wt.% respectively and kaolin with chemical composition $Al_2Si_2O_5(OH)_4$ were obtained from Aldrich. The copolymer was used after drying under vacuum at 50–52 °C for 24 h. DMSO was procured from Riedel-de Haen and used as received. Tetrahydrofuran (THF) purchased from Merck was first distilled at constant boiling temperature, followed by the addition of anhydrous calcium oxide left overnight. After distillation, it was refluxed over sodium wire with benzophenone as an indicator. The deep blue color of the solution confirmed the drying of THF, which was then collected and used as solvent.

2.2. Intercalation of kaolinite with DMSO

Modification of kaolinite was carried out with DMSO as a swelling agent. For this purpose, kaolinite (3 g) was charged into the round bottom flask and then mixed with DMSO (60 ml). The reaction mixture was agitated at 80 °C for 120 h. The modified clay mineral was filtered and washed with methanol to ensure the complete removal of excess DMSO. Modified kaolinite was dried in vacuum oven at 100 °C for 24 h. The dried cake was ground and screened with a 50 μm sieve. The modified kaolinite was labeled as K-DMSO and employed in the preparation of nanocomposites.

2.3. Preparation of nanocomposites

Nanocomposites were prepared by mixing appropriate amounts of K-DMSO and copolymer solution. For this purpose, a stock solution of the copolymer was prepared in dried THF (100 g) by dissolving 12 g of copolymer. For a particular concentration of nanocomposite fabrication, a known amount of the copolymer solution was taken in 50 ml flask and then stoichiometric amount of modified kaolinite was added. The resulting solution was agitated for 24 h at 25 °C. Similar procedure was followed for the preparation of other compositions of hybrids with different clay content. Thin films were cast in clean glass petri dishes by placing them on a leveled surface. Solvent evaporation was carried out at 40 °C for 24 h. These hybrid films obtained were then further dried in vacuum for 20 h in order to remove the solvent completely up to a constant weight.

2.4. Characterization

UV–vis transmission spectra of the pure copolymer and composite films were recorded using Shimadzu Spectrophotometer. The structural elucidation of copolymer matrix, kaolinite, K-DMSO and thin nanocomposite films was carried out by using Excalibur series Thermo Nicolet 6700 FTIR spectrophotometer, over the range of 4000–500 cm^{-1} in the ATR mode. The diffraction behavior of neat kaolinite, K-DMSO and nanocomposites was studied using X-ray diffractrometer Model XPert Pro 3040/60 PANALYTICAL with Ni-filtered Cu Kα radiation (40 kV, 30 mA). The scanning angle for all measurements was kept between $2\theta = 5°$ and 50°. The morphology of copolymer/kaolinite nanocomposites was investigated by recording the images using FEI Tecnai G2 Spirit Twin transmission electron microscope, operated at an accelerating voltage of 120 kV. The nanocomposite films were first microtomed into 30 nm ultra thin sections with the help of diamond knife using Leica Ultracut UCT ultramicrotome. SEM images of powdered kaolinite sample and cryo-fractured composite films were recorded with the help of scanning electron microscope Model JEOL JSM-6490LA operated at 20 kV. Tensile properties of the nanocomposite films were measured according to DIN procedure 53455 using Testometric Universal Testing Machine M500-30, and an average value obtained from five to seven different measurements in each case has been reported. Thermal stability of the nancomposites was determined using NETZSCH TG 209F3 thermogravimetric analyzer by using 1–5 mg of the sample in Al_2O_3 crucible heated from 25 to 900 °C at a heating rate of 10 °C/min under nitrogen atmosphere with a gas flow rate of 20 ml/min. The water uptake of these materials was carried out under the specifications of ASTM D570-81. Pure copolymer and nanocomposite films were first oven dried, cut to equal dimensions and then weighed to get the initial weight (W_o). The films were immersed in deionized water at 25 °C. After every 24 h, the films were taken out from water and were placed between the sheets of the filter paper to remove excess water and then weighed instantly. The films were again dipped in water and the process of weighing was repeated after every 24 h until the films reached constant weight (W_f). The total soaking time was 96 h because it was found to be enough for attaining equilibrium. The percent increase in weight of the films was calculated by using the formula $(W_f - W_o) / W_o$.

3. Results and discussion

The pure copolymer film obtained was transparent and the hybrid films were transparent to opaque with whitish color. The films became semitransparent and opaque as well as brittle with higher K-DMSO content. The mechanical behavior of hybrid films was recorded at ambient temperature. The average stress values of 5–7 samples were reported taking pure polymer as a reference for this study. Different techniques such as FTIR, XRD, TEM, SEM, TGA and mechanical testing were used to characterize these materials and results are reported.

3.1. Optical properties

The pure PVC–PVAc–PVA and copolymer/K-DMSO nanocomposite films were subjected for optical measurements. The pure copolymer film was transparent while its hybrid films were transparent to opaque and whitish in color. More quantitatively, transmittance was measured in the region 190–800 nm and transmission spectra of these nanomaterials are given in Fig. 1. The color of the composites films became whitish with increase of K-DMSO content, and the films beyond 4-wt.% clay mineral were semitransparent and even opaque at higher K-DMSO loading. The pure copolymer has a higher UV–vis transmission than the nanocomposites exhibiting more clarity and hence is more transparent whereas, hybrid films at higher kaolinite loading display lower optical clarity indicating strong scattering of kaolinite resulting in lower transparency. The transparency of these nanocomposites depends on the size, size distribution, and spatial distribution of the clay mineral in the copolymer matrix. Films containing up to 4-wt.% kaolinite were transparent, perhaps the average particle size was less than the wavelength of light, and the uniform dispersion of the clay mineral. However, at high K-DMSO loading, agglomeration of the kaolinite platelets occurred that decreased homogeneity causing opaqueness and brittleness, thus scattering more light, reducing transmittance and optical clarity.

3.2. FTIR spectroscopy

Various OH stretching vibrations illustrate the hydroxyl groups present on the interlayer surfaces. Actually, the surface hydroxyl groups provide evidence about the structural changes going on in the interlayer space. The introduction of organic modifiers into kaolinite developed interaction with surface hydroxyl groups of the clay mineral. Four kinds of bands were observed in kaolinite due to surface hydroxyl groups. The FTIR spectra of the hydroxyl stretching vibrations for neat kaolinite, K-DMSO are shown in Fig. 2. The band appeared at 3619 cm^{-1} was attributed due to the stretching vibrations of the internal hydroxyl group, while the bands at 3693, 3664 and 3651 cm^{-1} assigned to interlayer hydroxyl stretching. After intercalation of kaolinite with DMSO, the additional bands at 3534 and 3502 cm^{-1} observed are due to the hydrogen bonding between the DMSO and kaolinite, while 3693, 3664 and 3651 cm^{-1} are modified. The intensity of 3696 cm^{-1} band decreased while the intensity of stretching vibration of kaolinite at 3619 cm^{-1} remained unaffected. The band at 3660 cm^{-1} attributed to the hydroxyl stretching vibration of surface hydroxyl groups and band at 903 cm^{-1} was the hydroxyl deformation of surface hydroxyl groups that were hydrogen bonded to the —S=O group of DMSO. The structural analysis of pure copolymer matrix, kaolinite, K-DMSO and nanocomposite films containing 3 and 4-wt.% clay mineral are shown in Fig. 3. Other stretching vibrations of kaolinite appeared for Si—O at 1114, 1027 cm^{-1} (Zhang et al., 2007) and O—Al—OH at 788, 750, and 675 cm^{-1}. The PVC–PVAc–PVA exhibited a broad band in between

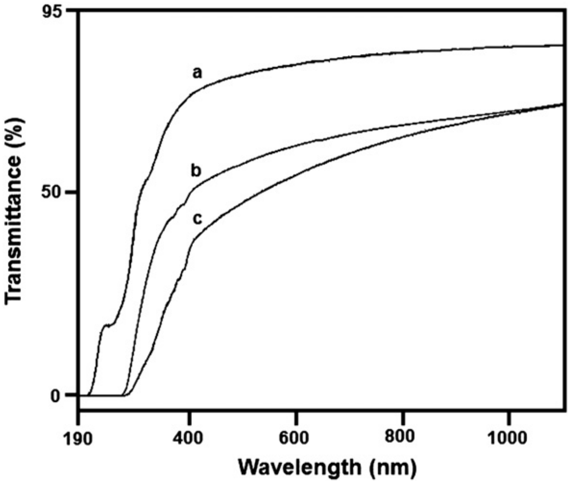

Fig. 1. UV–vis transmittance spectra of (a) pure copolymer, (b) 3-wt.%, and (c) 4-wt.% of K-DMSO in the nanocomposites.

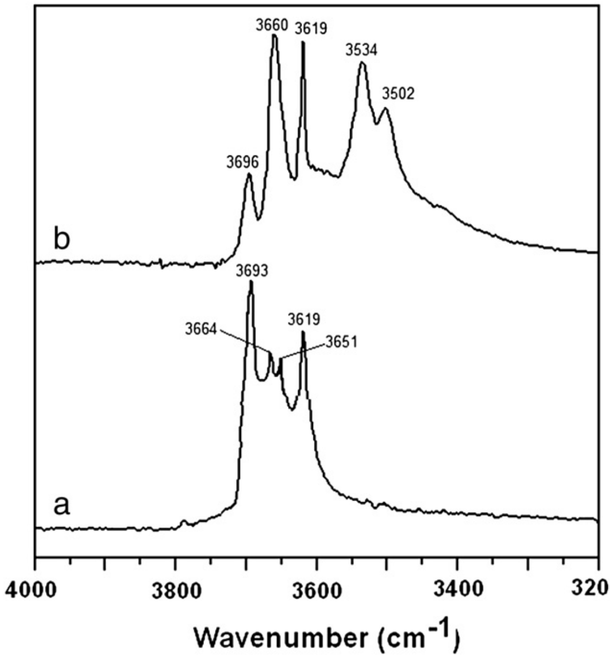

Fig. 2. FTIR spectra of (a) pure kaolinite and (b) K-DMSO.

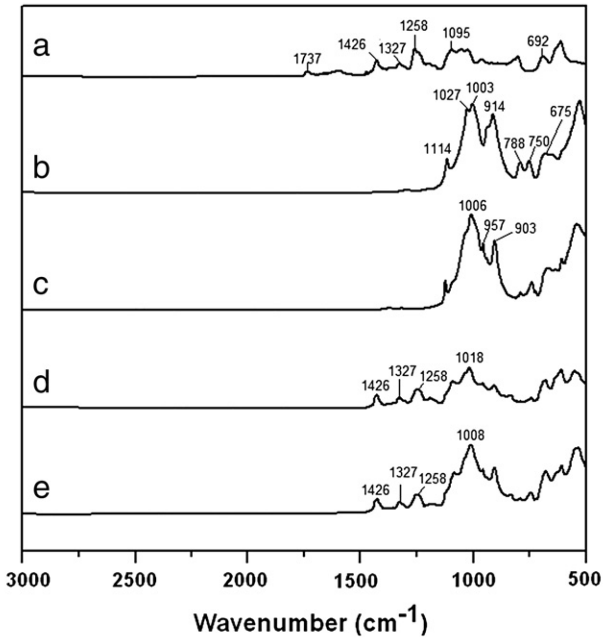

Fig. 3. FTIR spectra of (a) pure copolymer, (b) kaolinite, (c) K-DMSO, (d) 3-wt.% & (e) 4-wt.% K-DMSO in the nanocomposites.

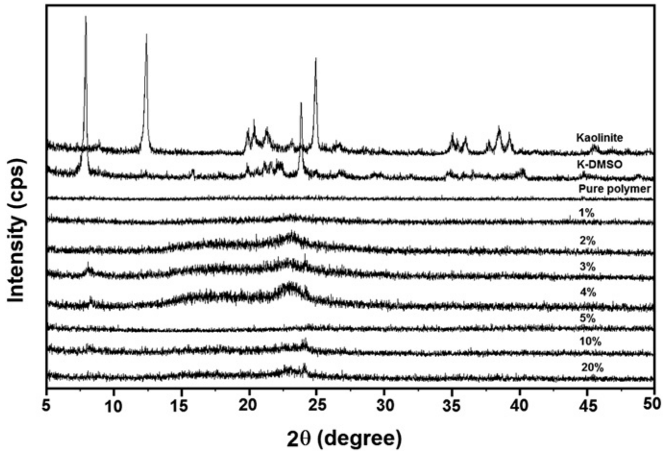

Fig. 4. XRD patterns of kaolinite, K-DMSO, pure copolymer and its nanocomposites.

3300 and 3500 cm^{-1} indicating the presence of OH groups in the copolymer. Aliphatic C—H stretching due to C—H and C—Cl appeared at 2962, 2914 and 2855 cm^{-1} and C—H bending at 1426, 1327 and 1258 cm^{-1}, C═O stretch at 1737 cm^{-1}, C—O stretch at 1095 cm^{-1} and C—Cl rocking at 692 cm^{-1}. The spectra of nanocomposites containing 3 and 4-wt.% kaolinite content showed the bands of copolymer/K-DMSO such as vibration at 1426 cm^{-1} assigned to the wagging of the methylene groups and at 1327 and 1258 cm^{-1} due to C—H deformation of CHCl group.

3.3. X-ray diffraction

XRD gives information about the change in d-spacing of clay mineral as a result of intercalation and the expansion achieved after nanocomposite formation due to inclusion of polymer within the kaolinite interlayers. The XRD of conventional composites usually show no change in the d-spacing due to poor dispersion of clay mineral within the polymer matrix. The shift of 2θ towards low value is the clear indication of intercalated structure, while the absence of any peak or broadening of peak implies exfoliated/intercalated structure due to the disruption of clay mineral within the polymer matrix. Diffractrograms of pure kaolinite, K-DMSO and nanocomposites are shown in Fig. 4. The XRD pattern of kaolinite shows a sharp peak at $2\theta = 12.42°$ ($d = 0.71$ nm) which shifted to a new peak position after treatment with DMSO $2\theta = 7.94°$ corresponding to a d-value of 1.1 nm. Moreover, the intensity of the K-DMSO peak becomes stronger indicating much ordered kaolinite layers. They are in good agreement with the literature values (Letaief and Detellier, 2007). Pure copolymer gave no diffraction peak which shows that it has an amorphous structure. After mixing K-DMSO with copolymer, the diffraction peaks disappeared in all the nanocomposites, which clearly suggested the disruption of ordered layers in the copolymer. Similar trend has been reported with PVC–kaolinite

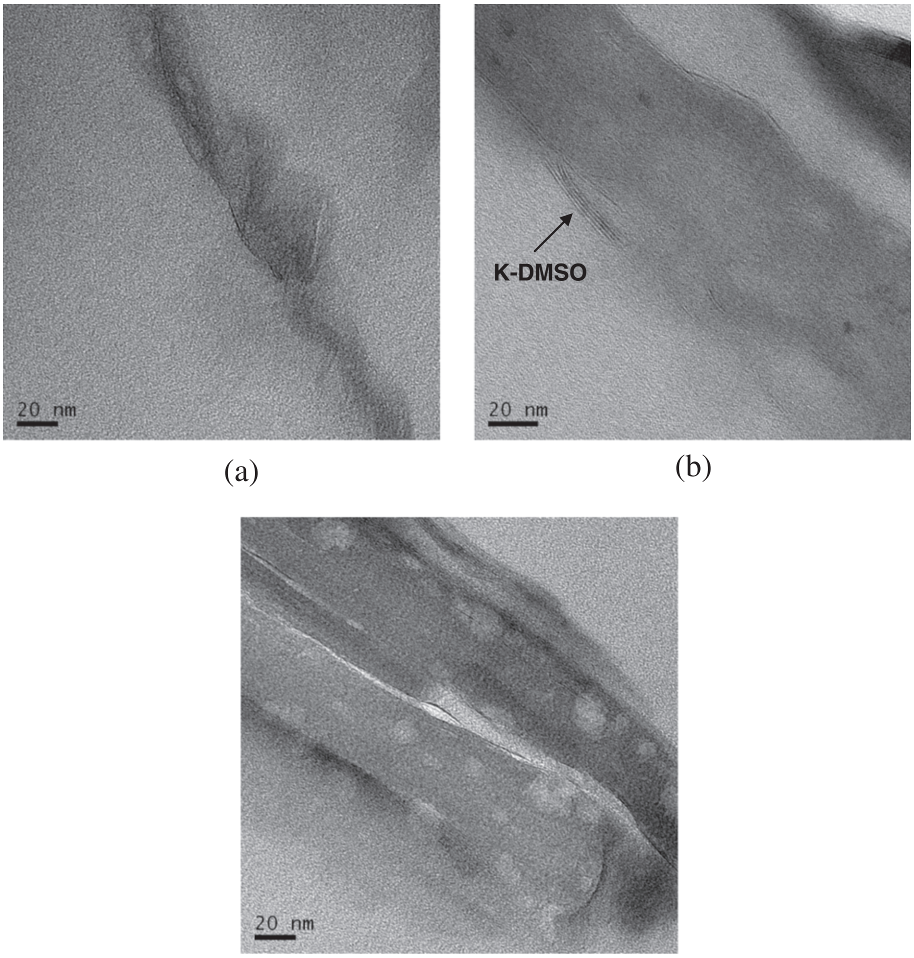

(a) (b)

(c)

Fig. 5. TEM micrographs of copolymer/K-DMSO nanocomposites: (a) 1-wt.%, (b) 5-wt.%, and (c) 10-wt.%.

nanocomposites (Turhan et al., 2010). So, disappearance of the typical diffraction peaks of kaolinite might indicate exfoliation or a too low concentration of K-DMSO in the nanocomposites.

3.4. Microscopic studies

The dispersion of kaolinite layers can be observed more clearly by scrutinizing images of ultrathin samples under TEM as XRD pattern gave incomplete information about the level of dispersion including no peak representing delaminated clay. Therefore, the internal morphology of the nanocomposites was monitored by TEM. Transmission electron micrographs of copolymer/K-DMSO nanocomposites are shown in Fig. 5. The micrographs displayed individual crystallites of the silicate which are visible as regions of alternating narrow, dark, and light bands revealing a strip distribution of silicate layers. Fig. 5a, b and c presents the complete disruption of 1, 5 and 10-wt.% of ordered K-DMSO in the nanocomposites. The interlayer distances between kaolinite layers appeared to range from 9 to 16 nm for 5-wt.% clay loading in the composites that is greater than the original space 1.1 nm between the layers of K-DMSO (Fig. 5b). The average interlayer distance was found to be 12 nm (±2.5). This proves that kaolinite layers have been dispersed in the copolymer matrix and nanocomposites have been formed. When the concentration of K-DMSO in the copolymer augmented to 10-wt.%, the interlayer distance between nanolayers was 6–14 nm, rather smaller than 5-wt.% kaolinite loading. The average interlayer distance obtained was 9 nm (±2.6) giving disordered and delaminated nanomaterials as shown in Fig. 5c. When copolymer entered the interlayers of clay mineral, it ruptured the original ordered structure of kaolinite yielding delaminated/intercalated nanocomposite morphology. These morphological results are in good agreement with the XRD patterns. SEM micrographs of powdered kaolinite and nanocomposite films are presented in Fig. 6. The micrographs of kaolinite showed fine grain particles while the nanocomposite images depicted even distribution of kaolinite in the copolymer matrix with very little or no agglomeration. The nanocomposite samples clearly presented a dispersed morphology and did not exhibit inorganic domains, suggesting well distributed K-DMSO in the copolymer matrix.

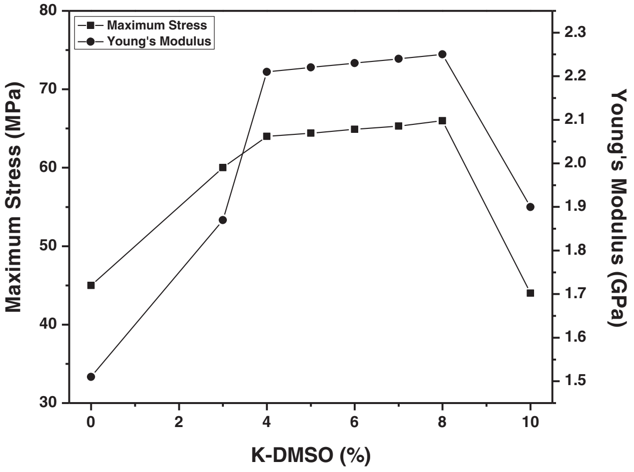

Fig. 7. Variation of max. stress and modulus Vs kaolinite content in the nanocomposites.

3.5. Mechanical properties

Tensile behavior of the system was investigated and various mechanical parameters obtained are illustrated in Figs. 7 & 8. The tensile strength of hybrid material increased up to 8-wt.% (66 MPa) relative to the pure copolymer (45 MPa) and then decreased with further incorporation of K-DMSO. The tensile modulus increased up to 8-wt.% hybrids, and then decreased with further addition of clay mineral (Fig. 7). Mechanical data revealed improvements in the tensile strength of the hybrid materials because the stress is more efficiently transferred from the polymer matrix to the inorganic filler. The interaction between matrix and filler resulted in mechanically stronger nanocomposites.

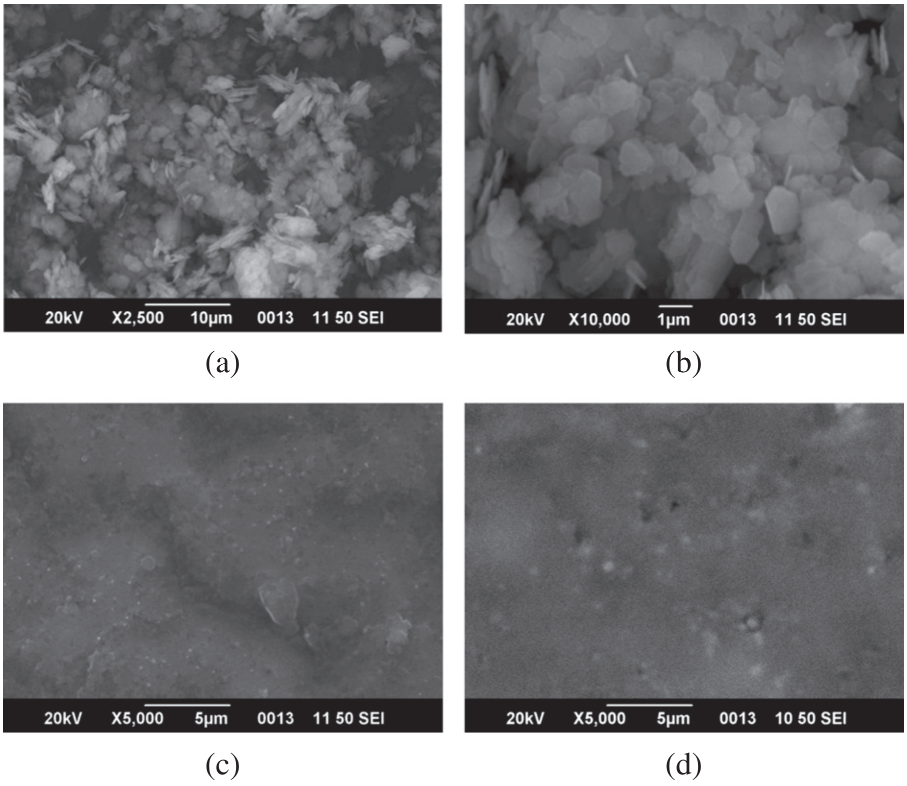

(a) (b)

(c) (d)

Fig. 6. SEM micrographs of (a & b) kaolinite, (c) 1-wt.% and (d) 5-wt.% of K-DMSO in the nanocomposites.

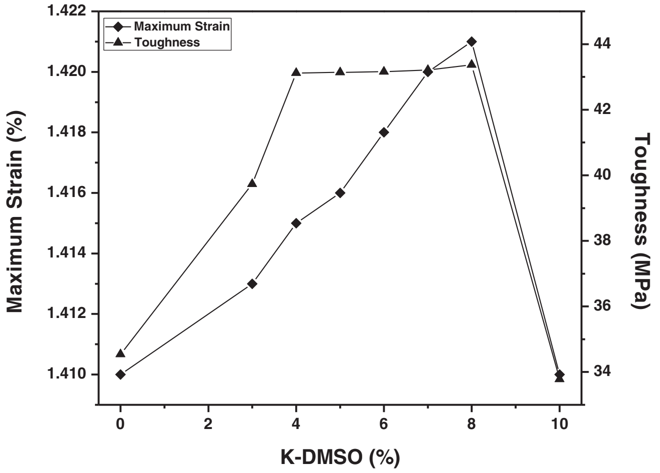

Fig. 8. Variation of strain and toughness Vs kaolinite content in the nanocomposites.

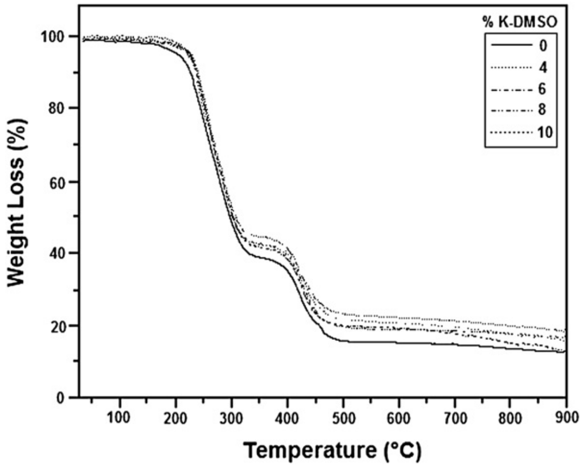

Fig. 9. TGA curves of (0) pure copolymer, 4, 6, 8 & 10-wt.% K-DMSO in nanocomposites.

Enhancement in modulus resulted due to strong interactions between the polymer matrix and clay mineral. Nevertheless upon high loading of silicate layers may stack together in the form of crystallites and interlayer spaces do not expand much, limiting the diffusion of the polymer chains and deteriorating the mechanical properties. The comparison of K-DMSO loading as a function of Young's modulus of different nanocomposites revealed that addition of clay mineral increased the modulus of the materials. An increasing trend is observed up to 8-wt.% clay loading. This behavior can be explained on the basis of strong interaction between modified kaolinite and copolymer. On further addition of K-DMSO the modulus decreased, which may be explained on the basis of formation of aggregates due to lesser kaolinite polymer interactions as was evident from TEM results (Fig. 5). Similar results were observed for the maximum strain and toughness (Fig. 8), i.e. increased up to 8-wt.% clay mineral and then decreased beyond its further addition. Improvement of mechanical properties of EPDM/kaolinite nanocomposites showed a two fold increase in tensile strength upon 7-wt.% addition of kaolinite relative to the neat EPDM. Elongation at break of composite films initially decreased with kaolinite content and then displayed a steady increase. The tensile modulus of the composites also exhibited a similar trend as that of the tensile strength. The enhancement in tensile strength and tensile modulus is the direct manifestation of the dispersion of kaolinite layers in the EPDM matrix and the strong interaction between EPDM (Mon et al., 2011).

3.6. Thermogravimetric analysis

Thermogravimetric analysis was carried out to compare the thermal stability of copolymer/K-DMSO composites and thermograms are given in Fig. 9. The thermal degradation of copolymer nanocomposites occurred through two degradation steps. The first step corresponds to the weight loss caused by dehydration and dehydrochlorination of PVC–PVA–PVAc while the second step presents the total weight loss resulted from the degradation of the residuals. The pure copolymer was decomposed around 262 °C while nanocomposites containing 10-wt.% K-DMSO showed a decomposition temperature around 293 °C. The thermal degradation temperature of nanocomposites was shifted to higher temperature as compared to pure polymer. The interactions between polymer and clay mineral showed that addition of kaolinite in the matrix reduced the degradation of polymer and organophilic treatment improved compatibility between the phases and subsequently the thermal stability of nanocomposites. Thus, the degradation of polymer was hindered and the thermal stability of copolymer composite increased. The residual weight loss is roughly proportional but does not correspond to the clay ratio introduced in to the nanocomposites due to the loss of water from the kaolinite at high temperature.

3.7. Water absorption measurements

The water uptake of pure copolymer and nanocomposite materials measured under the saturation conditions (96 h) are presented in Fig. 10. The results revealed the highest water absorption for the pure copolymer film (6%) due to exposure of hydrophilic polar groups to the surface of copolymer where water molecules developed secondary bond forces with these polar groups. The increase in weight of the nanocomposite films due to uptake of water gradually decreased as the K-DMSO content in nanocomposites increased, even 10-wt.% loading of K-DMSO reduced the water absorption up to 0.1%. This reduction is apparently due to the mutual interaction between the organic and inorganic phases which leads to lesser availability of acetate and hydroxyl groups of copolymer to interact with water. The kaolinite layers created a tortuous path, which hindered the diffusion pathways through the nanocomposites.

4. Conclusions

Intercalation of kaolinite with DMSO changed the basal spacing of kaolinite, and it expanded from 0.712 to 1.12 nm suggesting enhanced organophilicity of kaolinite. A series of nanocomposite materials consisting of polymer and kaolinite were prepared by effectively dispersing of clay mineral in the copolymer matrix by solution intercalation method. XRD, TEM, and TGA experiments were carried out to

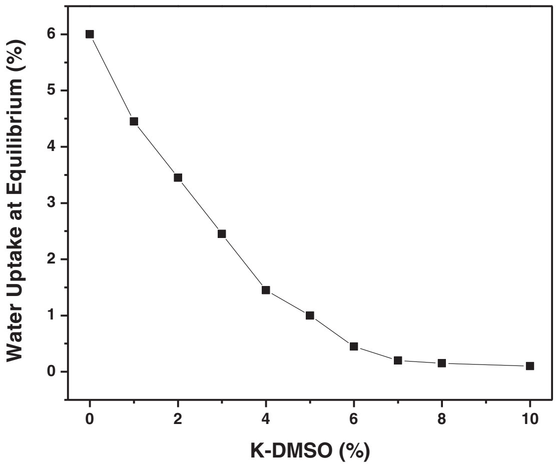

Fig. 10. Water uptake of copolymer/K-DMSO nanocomposites.

characterize the morphology and properties of the nanocomposites. Incorporation of kaolinite into polymer resulted in an increase in thermal stability. Thermograms showed high thermal stability of polymer–kaolinite nanocomposite relative to the pure polymer. TEM results were in accordance with those of XRD and tensile testing gave improved mechanical properties. Water uptake data indicated improved barrier properties of the nanomaterials.

References

Alexandre, M., Dubois, P., 2000. Polymer-layered silicate nanocomposites: preparation, properties, and uses of a new class of materials. Mater. Sci. Eng. 28, 1–63.

Alkan, M., Demirbas, O., Dogan, M., 2005. Electrokinetic properties of kaolinite in mono- and multivalent electrolyte solutions. Microporous Mesoporous Mater. 83, 51–59.

Alkan, M., Kalay, B., Dogan, M., Demirbas, O., 2008. Removal of copper ions from aqueous solutions by kaolinite and batch design. J. Hazard. Mater. 153, 867–876.

Alvi, M.U., Zulfiqar, S., Yavuz, C.T., Kweon, H.-S., Sarwar, M.I., 2013. Influence of aminosilane coupling agent on aromatic polyamide/intercalated clay nanocomposites. Ind. Eng. Chem. Res. 52, 6908–6915.

Alvi, M.U., Zulfiqar, S., Yavuz, C.T., Kweon, H.-S., Sarwar, M.I., 2014. Nanostructure and mechanical properties of aromatic polyamide and reactive organoclay nanocomposites. Mater. Chem. Phys. 147, 636–643.

Bailey, S.W., 1988. Hydrous Phyllosilicates. American Mineralogical Society, Washington DC.

Cabeda, L., Gimenez, E., Lagoron, J.M., Gavara, R., Saura, J.J., 2004. Development of EVOH–kaolinite nanocomposites. Polymer 45, 5233–5238.

Elbokl, T.A., Detellier, C., 2008. Intercalation of cyclic imides in kaolinite. J. Colloid Interface Sci. 323, 338–348.

Frost, R.L., Kristof, J., Horvath, E., Kloprogge, J.T., 1999. Modification of kaolinite surfaces through intercalation with potassium acetate. J. Colloid Interface Sci. 214, 109–117.

Karaoglu, M.H., Dogan, M., Alkan, M., 2009. Removal of cationic dyes by kaolinite. Microporous Mesoporous Mater. 122, 20–27.

Komori, Y., Sugahara, Y., Kuroda, K., 1998. A kaolinite–NMF–methanol intercalation compound as a versatile intermediate for further intercalation reaction of kaolinite. J. Mater. Res. 13, 930–934.

Ledoux, R.L., White, J.L.J., 1996. Infrared studies of hydrogen bonding interaction between kaolinite surfaces and intercalated potassium acetate, hydrazine, formamide, and urea. J. Colloid Interface Sci. 21, 127–152.

Letaief, S., Detellier, C., 2007. Nanohybrid materials from the intercalation of imidazolium ionic liquids in kaolinite. J. Mater. Chem. 17, 1476–1484.

Letaief, S., Diaco, T., Pell, W., Gorelsky, S.I., Detellier, C., 2008. Ionic conductivity of nanostructured hybrid materials designed from imidazolium ionic liquids and kaolinite. Chem. Mater. 20, 7136–7142.

Li, Y., Zhang, B., Pan, X., 2008. Preparation and characterization of PMMA–kaolinite intercalation composites. Compos. Sci. Technol. 68, 1954–1961.

Mbey, J.A., Hoppe, S., Thomas, F., 2012. Cassava starch–kaolinite composite film, effect of clay content and modification on film properties. Carbohydr. Polym. 88, 213–222.

Mon, S.G., Ruban, Y.J.V., Roy, D.V., 2011. Synthesis of kaolinite-filled EPDM rubber composites by solution intercalation: structural characterization and studies on mechanical properties. Appl. Nanosci. 1, 131–135.

Pinnavaia, T.J., Beall, G.W., 2000. Polymer–clay nanocomposites. Wiley Series in Polymer ScienceWiley, Chichester, U.K.

Ruiz-Hitzky, E., Meerbeek, A.V., 2006. Clay mineral– and organoclay–polymer nanocomposite. In: Bergaya, F., Theng, B.K.G., Lagaly, G. (Eds.), Handbook of Clay Science. Developments in Clay in Science 1. Elsevier, Amsterdam, pp. 583–621.

Theng, B.K.G., 1979. Formation and properties of clay–polymer complexes. Developments in Soil Science 9. Elsevier, Amsterdam.

Tomposon, J.G., Cuff, C., 1985. Crystal structure kaolinite: dimethyl sulfoxide intercalate. Clay Clay Miner. 33, 490–500.

Tonle, I.K., Diaco, T., Ngameni, E., Detellier, C., 2007. Nanohybrid kaolinite-based materials obtained from the interlayer grafting of 3-aminopropyltriethoxysilane and their potential use as electrochemical sensors. Chem. Mater. 19, 6629–6636.

Turhan, Y., Dogan, M., Alkan, M., 2010. Poly(vinyl chloride)/kaolinite nanocomposites: characterization and thermal and optical properties. Ind. Eng. Chem. Res. 49, 1503–1513.

Uwins, P.J.R., Mackinnon, I.D.R., Thompson, J.G., Yago, A.J.E., 1993. Kaolinite–NMF intercalates. Clay Clay Miner. 41, 707–717.

Viville, P., Lazzaroni, R., Pollet, E., Alexandre, M., Dubois, P., Borcia, G., Pireaux, J.-J., 2003. Surface characterization of poly(ε-caprolactone)-based nanocomposites. Langmuir 19, 9425–9433.

Zahra, M., Zulfiqar, S., Yavuz, C.T., Kweon, H.-S., Sarwar, M.I., 2014. Conductive nanocomposite materials derived from SEBS-g-PPy and surface modified clay. Compos. Sci. Technol. 100, 44–52.

Zhang, B., Li, Y., Pan, X., Jia, X., Wang, X., 2007. Intercalation of acrylic acid and sodium acrylate into kaolinite and their in situ polymerization. J. Phys. Chem. Solids 68, 135–142.